

Letters 18, 1029 (1967).

¹²J. J. Sakurai, Phys. Rev. Letters 19, 803 (1967); A. Dar, to be published.

¹³S. Weinberg, Phys. Rev. Letters 18, 507 (1967).

¹⁴T. Das, G. S. Guralnik, V. S. Mathur, F. E. Low, and J. E. Young, Phys. Rev. Letters 18, 759 (1967).

¹⁵Saturating the $T=Y=0$ spectral-function sum rules with ω , φ , D , and E , we obtain the result

$$m^{-2}(D) \cos^2\theta + m^{-2}(E) \sin^2\theta = [1 - (F_\eta^2 + F_{\eta'}^2) / 2F_\pi^2] \times [m^{-2}(\omega) \cos^2\theta' + m^{-2}(\varphi) \sin^2\theta'],$$

where θ and θ' are unknown angles. This gives the inequality

$$0.74F_\pi^2 \leq (F_\eta^2 + F_{\eta'}^2) \leq 1.38F_\pi^2.$$

Combined with Eq. (26) and the mixed-channel formula of Ref. 8, this inequality provides the upper bound $\mu_\kappa \leq 1410$ MeV. But it is again clear that the heavier κ mass may only be realized with very large SU(3) breaking (e.g., $F_{\eta'}^2 > 2F_\eta^2$).

¹⁶The equality $\mu_{K^*}^2 - \mu_\pi^2 = m^2(K^*) - m^2(\rho)$ is both mysterious and well satisfied. Its natural generalization to even parity states is $\mu_\kappa^2 = m^2(K_A) - m^2(A_1)$ and yields $\mu_\kappa = 620$ MeV.

EXPERIMENTAL TESTS OF THE VECTOR-DOMINANCE MODEL*†

J. G. Asbury,‡ U. Becker, William K. Bertram,§ M. Binkley, E. Coleman,|| C. L. Jordan, M. Rohde, A. J. S. Smith,** and Samuel C. C. Ting

Deutsches Elektronen-Synchrotron, Hamburg, Germany, and

Department of Physics and Laboratory of Nuclear Science, Massachusetts Institute of Technology, Cambridge, Massachusetts

(Received 2 January 1968)

In this Letter we report the results of an experiment designed to perform some independent tests of the validity of the vector-dominance model¹ of electromagnetic interactions of hadrons. The vector-dominance model relates the electromagnetic current $J_\mu(x)$ of hadrons with the phenomenological fields of vector mesons $\rho_\mu(x)$, $\varphi_\mu(x)$, and $\omega_\mu(x)$ via

$$J_\mu(x) = -\frac{m_\rho^2}{2\gamma_\rho} \rho_\mu(x) - \frac{m_\omega^2}{2\gamma_\omega} \omega_\mu(x) - \frac{m_\varphi^2}{2\gamma_\varphi} \varphi_\mu(x). \quad (1)$$

It follows from (1) that the electromagnetic form factors of nucleons and pseudoscalar mesons as well as electromagnetic decays of mesons can all be expressed in terms of measurable quantities γ_ρ , γ_ω , and γ_φ , which couple the vector meson to the photon. In particular, the photoproduction of ρ^0 mesons on complex nuclei can be thought of as via the diagram² (Fig. 1) where the photon materializes itself

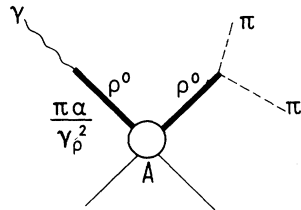


FIG. 1. Feynman diagram for photoproduction of ρ^0 on complex nuclei.

into ρ^0 with a coupling strength $\alpha\pi/\gamma_\rho^2$ and the ρ^0 meson subsequently scatters diffractively off the whole nucleus. This diagram for photoproduction of ρ^0 mesons then carries the following two important implications.

(I) A factor $-m^{-2}$ enters from the ρ^0 propagator and the ρ^0 decay spectrum can be shown² to be of the form

$$R(m) = (m_\rho/m)^4 f_{\text{BW}}(m) \cdots, \quad (2)$$

where $m^2 = p_{\pi^+} + p_{\pi^-}$, and where $f_{\text{BW}}(m)$ is the relativistic Breit-Wigner mass formula for the decay³ $\rho^0 \rightarrow \pi^+\pi^-$:

$$f_{\text{BW}}(m) = \frac{1}{\pi} \frac{m \Gamma(m)}{(m_\rho^2 - m^2)^2 + m_\rho^2 \Gamma^2(m)}, \quad (3)$$

with

$$\Gamma(m) = \frac{\rho}{m} \left[\frac{(\frac{1}{2}m)^2 - m_\pi^2}{(\frac{1}{2}m_\rho)^2 - m_\pi^2} \right]^{3/2} \Gamma_0.$$

Equation (2) provides a mass shift of ≈ 20 MeV/ c^2 and has been used as an explanation for the difference between the mass $m_\rho = 765$ MeV/ c^2 (ρ^0 mesons produced from πN interactions⁴) and that of $m_{\rho'} = 740$ MeV/ c^2 (ρ^0 mesons produced in photoproduction experiments⁵).

The first purpose of the present experiment is to study the spectrum of $\rho - \pi^+\pi^-$ in the region of high $\pi^+\pi^-$ invariant mass, $930 < m < 1130$

MeV/c², where $(m_\rho/m)^4 \ll 1$. Hence, a comparison of the spectrum $R(m)$ with the experimental data provides a very sensitive test of the validity of Eq. (2).

(II) Following from the diagram of Fig. 1 and the experimental result² that the forward ρ^0 production amplitude on complex nuclei proceeds via a purely imaginary amplitude, the cross section $d\sigma(\gamma A \rightarrow A\rho^0)/d|t|$ is related to the total ρ -nucleus cross section $\sigma_T(\rho A \rightarrow \rho A)$ via

$$\left. \frac{d\sigma(\gamma A \rightarrow \rho^0 A)}{d|t|} \right|_{t \rightarrow 0} = \frac{1}{16} \frac{k}{p_\rho} \frac{\alpha}{\gamma_\rho^2} \sigma_T^2(\rho A \rightarrow \rho A), \quad (4)$$

where k = incident photon energy, $\alpha = 1/137$, $t = (k - p_{\pi^+} - p_{\pi^-})^2$, and p_ρ = the outgoing ρ^0 momentum.

If the nucleus is represented as a purely absorptive medium of density distribution $\rho(r) = \rho = \text{constant}$ for $r < r_0 A^{1/3} = R$ and $\rho(r) = 0$ elsewhere, then in the simplified eikonal approximation of Drell and Trefil⁶ the total cross section can be expressed as an integral over b , the impact parameter:

$$\sigma_T = 4\pi \int_0^R b db [1 - \exp(-\sigma_{\rho N} \int_0^z \rho dz)], \quad (5)$$

where $r^2 = b^2 + z^2$ and $\sigma_{\rho N}$ is the total ρ -nucleon cross section which can be determined from the relative yields of photoproduction of ρ^0 on complex nuclei.

The second purpose of the experiment is to measure precisely the forward photoproduction cross section of ρ^0 mesons on complex nuclei and thereby use Eqs. (4) and (5) to deduce the ρ^0 -photon coupling constant γ_ρ and to compare it with the value obtained directly from the measurement⁷ of the branching ratio $\Gamma(\rho \rightarrow e^+e^-)/\Gamma(\rho \rightarrow \pi^+\pi^-)$.

The experiment, performed at the Deutsches Elektronen-Synchrotron, used a double-arm magnetic spectrometer to detect the $\pi^+\pi^-$ pairs. The detailed features of this spectrometer have been described in previous Letters.⁸ A total of 1.5×10^4 events was taken in the invariant-mass region $400 < m < 930$ MeV/c² on C, Cu, and Pb nuclei, at $p_\rho = 4.500$ GeV/c, $k_0 = 6.02$ GeV; and a total of 5×10^4 events was taken in the invariant-mass region $930 < m < 1130$ MeV/c² on the C nucleus at $p_\rho = 5.000$ GeV/c and with $k_0 = 6.200$ GeV ($k_0 = \text{max energy of bremsstrahlung spectrum}$).

Before discussing the results of the present

experiment, it is helpful to recall the conclusions drawn from a previous experiment⁹ on photoproduction of ρ^0 mesons (in the $\pi^+\pi^-$ invariant-mass region $400 < m < 930$ MeV/c²) on complex nuclei. This experiment shows that high-energy ρ^0 photoproduction agrees with the predictions of diffraction production and that the cross section in the forward region can be described in the form

$$\frac{d^2\sigma}{d\Omega dm} = C \cdot 2mR(m)p^2 f'(p) f_T(R, t, \sigma_{\rho N}), \quad (6)$$

where the function f_T describes the production and reabsorption of ρ^0 meson by the target nucleus, $f'(p)$ describes the energy variation of the ρ^0 production cross section, and $R(m)$ is the spectrum function assumed to be (2). Comparing (6) with the relative A dependence of the production cross section yields $\sigma_{\rho N} = 31.3 \pm 2.3$ mb and $r_0 = 1.29 \pm 0.09$ F. For high energy and small momentum transfer Eq. (6) becomes

$$\frac{d^2\sigma}{d\Omega dm} = C \cdot 2mR(m)p^2 e^{at}, \quad (7)$$

where, with a carbon target, $C = (3.72 \pm 0.23)$ mb sr⁻¹ (GeV/c)⁻².

Typical results of the present experiment are shown in Fig. 2. To analyze the data and to compare the spectrum with Eq. (2), we group the events from the carbon target according to their invariant-mass distribution over (a) the mass region $400 < m < 930$ MeV/c², with a total of 7×10^3 events, and (b) the mass region $930 < m < 1130$ MeV/c², with a total of 5×10^4 events. To study the origin of the $\pi^+\pi^-$ spectrum in the high invariant-mass region, we compare the t dependence of the weighted cross section $[f'(p)]^{-1}(d\sigma/dt)$ for both the ρ^0 region of $720 < m < 820$ MeV/c² and the invariant-mass region of $930 < m < 1130$ MeV/c².

Figure 2(a) shows the agreement both in absolute value and slope between $d\sigma(t)/dt$ for the $\pi^+\pi^-$ spectrum above 930 MeV/c² and for $720 < m < 820$ MeV/c², where the ρ^0 meson is known to be diffracted off the whole nucleus. Both sets of data are consistent with $d\sigma/dt \propto e^{at}$, where $a = (47 \pm 5)$ (GeV/c)⁻². The similarity of t dependence of the cross sections gives strong indication that all the $\pi^+\pi^-$ pairs in the region $1130 > m > 930$ are indeed coming from ρ^0 mesons which decay into $\pi^+\pi^-$ pairs after being diffracted off the whole nucleus.

Having established that the high-invariant-

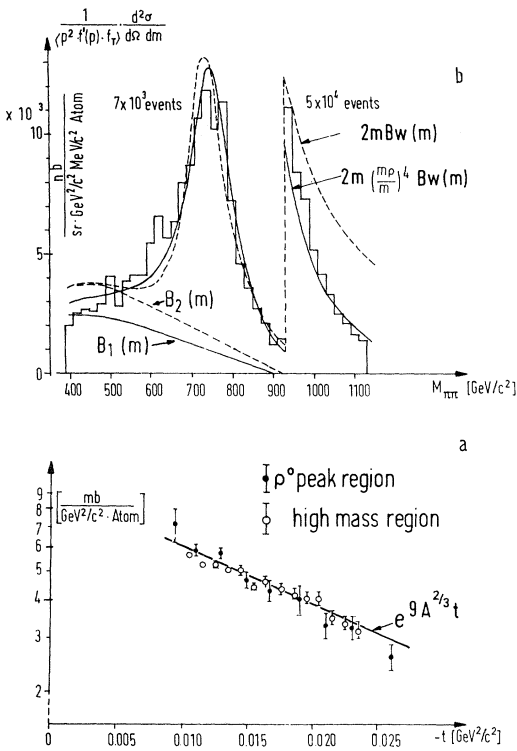


FIG. 2. (a) The quantity $[f'(p)]^{-1}d\sigma/d|t|$ is shown as a function of t , the square of the momentum transfer to the nucleus, for carbon target and for both the ρ^0 peak region ($720 < m < 820 \text{ MeV}/c^2$) and the high-mass region ($930 < m < 1130 \text{ MeV}/c^2$). The similarity of the t dependence between the two mass regions indicates that the $\pi^+\pi^-$ pairs in the high-invariant-mass region are from ρ^0 decay. (b) Pion-pair invariant-mass spectrum $[p^2 f'(p) f_T]^{-1} d^2\sigma/d\Omega dm$ in units of $\text{nb} (\text{GeV}/c)^{-2} (\text{MeV}/c^2)^{-1} \text{sr}^{-1} \text{atom}^{-1}$ for carbon target. In the mass region $400 < m < 930 \text{ MeV}/c^2$ the data were fitted to $U_1(m)$ (solid line) and $U_2(m)$ (dotted line) to determine the parameters m_ρ , Γ_0 . With the spectrum functions $2mR(m)$ and $2mf_{BW}(m)$ so determined, their behaviors over the region $1130 > m > 930 \text{ MeV}/c^2$ were then plotted ($\times 10$) and compared with the experimental data.

mass $\pi^+\pi^-$ pairs are from ρ^0 decay, we can now compare the data with the spectrum functions $R(m)$ and $f_{BW}(m)$. In each case the functions

$$U_1(m) = C_1 2mR(m) + B_1(m)$$

$$U_2(m) = C_2 2mf_{BW}(m) + B_2(m)$$

were first fitted to the data from the mass region $400 < m < 930 \text{ MeV}/c^2$ to determine the parameters Γ_0 and m_ρ . The function $B(m)$ is a phenomenological background function deter-

mined from the previous experiment⁹ to be a power series in m . The results of the best fitted values for the $2mR(m)$ distribution function are (as shown in the previous experiment⁹) $\Gamma_0 = 130 \pm 5 \text{ MeV}/c^2$, $m_\rho = 765 \pm 5 \text{ MeV}/c^2$, and for the $2mf_{BW}(m)$ distribution function, $\Gamma_0 = 104 \pm 15 \text{ MeV}/c^2$ and $m_\rho = 737 \pm 5 \text{ MeV}/c^2$.

With the spectrum functions $R(m)$ and $f_{BW}(m)$ determined, their behavior over the region $1130 > m > 930 \text{ MeV}/c^2$ was then computed and compared with the experimental data. As seen in Fig. 2(b), the data agree well with the distribution function $2mR(m)$ in both the shape and the normalization. But the data do not agree in any way with the relativistic Breit-Wigner decay distribution.

To deduce the value of $\gamma_\rho^2/4\pi$ from Eq. (4), the values of $[d\sigma(\gamma + A \rightarrow A + \rho^0)/d|t|]_{t \rightarrow 0}$ were obtained by studying the behavior of $d\sigma/d|t|$ as a function of t in the region $0.004 < |t| < 0.06 (\text{GeV}/c)^2$ for a fixed mass interval $700 < m < 800 \text{ MeV}/c^2$ and for target nuclei of C, Cu, and Pb. The values of $(d\sigma/d|t|)_{t \rightarrow 0}$ were obtained by extrapolating the data to $t = 0$. Using the values of $\sigma_{\rho N}$ and r_0 , determined from the previous experiment,⁹ we then calculate $\sigma_T(\rho A \rightarrow \rho A)$ with Eq. (5). The knowledge of σ_T and $(d\sigma/d|t|)_{t \rightarrow 0}$ allows us to determine the value $\gamma_\rho^2/4\pi$ from Eq. (4). In Table I, we list the values of σ_T on various nuclei as well as the value of $\gamma_\rho^2/4\pi$ determined by the above method. Thus the values of $\gamma_\rho^2/4\pi$ obtained according to the diagram of Fig. 1 are consistent with each other and are in good agreement with the values $\gamma_\rho^2/4\pi = 0.40^{+0.11}_{-0.99}$ determined directly from the branching-ratio experiment.⁷

In summary, the results of this experiment show that the $\rho^0 \rightarrow \pi^+\pi^-$ spectrum fits well with Eq. (2) and that the values of $\gamma_\rho^2/4\pi$ deduced from the particular production process agree with the value determined from direct branching-ratio measurement. Thus we conclude that the diagram of Fig. 1 is indeed the dominant diagram for photoproduction of ρ^0 on complex

Table I. Summary of coupling constants $\gamma_\rho^2/4\pi$ and the total ρ^0 -nucleus cross section σ_T .

| Nucleus | σ_T (b) | $\gamma_\rho^2/4\pi$ |
|---------|-------------------|----------------------|
| C | 0.26 | 0.49 ± 0.12 |
| Cu | 1.11 | 0.42 ± 0.10 |
| Pb | 2.90 | 0.40 ± 0.10 |

nuclei.

We wish to thank Professor W. Jentschke, Professor H. Joos, Professor V. F. Weisskopf, Professor A. G. Hill, and Professor P. Demos for the support which made this experiment possible. We acknowledge many interesting discussions with Professor D. Frisch, Professor G. Weber, and Professor L. Stodolsky. One of us (J.G.A.) would like to thank the High Energy Physics Division of Argonne National Laboratory for permission to participate in this experiment and, in particular he wishes to thank Professor T. H. Fields for support and encouragement.

*Accepted without review under policy announced in Editorial of 20 July 1964 [Phys. Rev. Letters **13**, 79 (1964)].

†Work supported in part by the Deutsches Elektronen-Synchrotron, the Volkswagenwerk Foundation, and the U. S. Atomic Energy Commission.

‡Present address: Argonne National Laboratory, Argonne, Ill.

§Present address: University of Illinois, Urbana, Ill.

||Present address: University of Minnesota, Minneapolis, Minn.

**Present address: Princeton University, Princeton, N. J.

¹M. Gell-Mann, D. Sharp, and W. G. Wagner, Phys. Rev. Letters **8**, 261 (1962); S. L. Glashow, Phys. Rev. Letters **7**, 469 (1961); Y. Nambu and J. J. Sakurai, Phys. Rev. Letters **8**, 79 (1962); N. M. Kroll, T. D. Lee, and B. Zumino, to be published; R. van Royan and V. F. Weisskopf, to be published; H. Joos, Phys. Letters **24B**, 103 (1967).

²M. Ross and L. Stodolsky, Phys. Rev. **149**, 1172 (1966); J. G. Asbury *et al.*, Phys. Rev. Letters **19**, 869 (1967).

³J. D. Jackson, Nuovo Cimento **34**, 1644 (1964).

⁴A. H. Rosenfeld *et al.*, Rev. Mod. Phys. **39**, 1 (1967).

⁵L. J. Lanzerotti *et al.*, Phys. Rev. Letters **15**, 210 (1965); Aachen-Berlin-Bonn-Hamburg-Heidelberg-München Collaboration, Nuovo Cimento **41A**, 270 (1966).

⁶S. D. Drell and J. S. Trefil, Phys. Rev. Letters **16**, 552, 832(E) (1966).

⁷S. C. C. Ting, Report to 1967 International Conference on Photons and Electrons, Stanford University, September, 1967 (unpublished).

⁸J. G. Asbury *et al.*, Phys. Rev. Letters **18**, 65 (1967).

⁹J. G. Asbury *et al.*, Phys. Rev. Letters **19**, 865 (1967).

PHOTOPRODUCTION OF π^0 IN THE BACKWARD DIRECTION*

G. Buschhorn, P. Heide, U. Kötz, R. A. Lewis,† P. Schmüser, and H. J. Skronn
Deutsches Elektronen-Synchrotron, Hamburg, Germany, and

II. Institut für Experimentalphysik der Universität Hamburg, Hamburg, Germany

(Received 30 October 1967)

The photoproduction of neutral pions in the reaction $\gamma p \rightarrow \pi^0 p$ has been investigated in the backward direction ($\theta_{\pi^0}^{\text{c.m.}} \approx 180^\circ$) at photon energies E_γ from 0.8 to 5.5 GeV, using a bremsstrahlung beam from the Deutsches Elektronen-Synchrotron (DESY) electron accelerator. Only the recoil proton was detected and its momentum determined with a magnetic spectrometer. Since the lab momentum of the recoil protons is 300-400 MeV/c higher than the momentum of light particles, it was possible to detect the protons in the forward direction without serious troubles from the high positron background.

The minimum energetic separation between single and multiple pion production processes is of the order of 40 MeV. Therefore, a good momentum resolution of the spectrometer was required.

The experimental setup is shown in Fig. 1. The photon beam was produced in a tungsten

target of 0.06 radiation lengths and defined by three lead collimators. The flux was measured with a gas-filled quantameter. The liquid hydrogen target had a length of 30 cm.

The spectrometer produced an angular focus

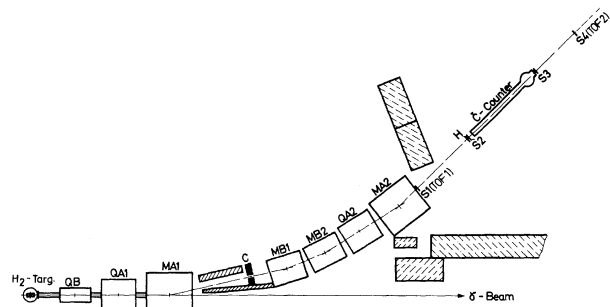


FIG. 1. Experimental setup: QB and QA, quadrupoles; MA and MB, bending magnets; C, lead collimator; S1, ..., S4 scintillation counters; H, hodoscope; S1 and S4, time-of-flight (TOF) counters.